Empirically Derived Effective Stiffness Expressions for Concrete Walls

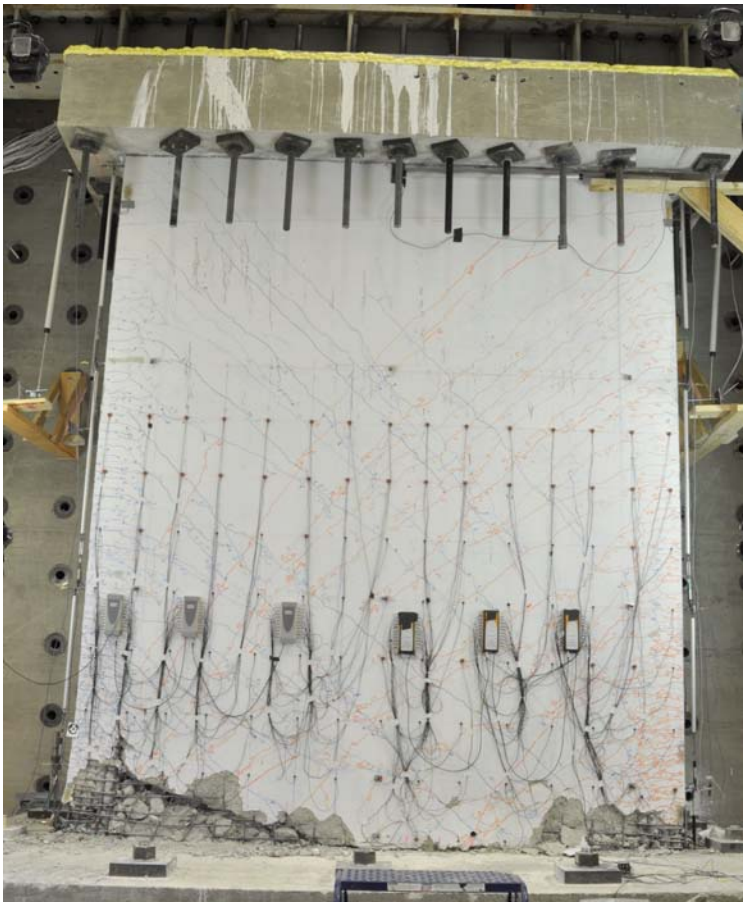

Andrew Mock, SCA Consulting Engineers
Anahid Behrouzi, Tufts University
Dr. Laura Lowes, University of Washington
Dr. Dawn Lehman, University of Washington
Dr. Daniel Kuchma, Tufts University

Funding provided by the **National Science Foundation** and the **Charles Pankow Foundation**

Empirically Derived Effective Stiffness Expressions for Concrete Walls

Andrew Mock, SCA Consulting Engineers
Anahid Behrouzi, Tufts University
Dan Kuchma, Tufts University
Laura Lowes and Dawn Lehman, University of Washington

1 Abstract

In most cases, analysis to determine component demands for seismic design of concrete buildings employs linear elastic models in which reduced, effective component stiffnesses are used. This document i) reviews the recommendations for defining the effective flexural, shear and axial stiffness of concrete walls that are included in current design codes, standards and guidelines and ii) compares these recommendations with stiffness expressions derived directly from experimental data by the authors and others. Section 2 reviews existing empirically derived and code-, standard-, and guideline-based expressions for the effective stiffness of concrete walls. Section 3 presents the process used by the authors to compute effective stiffness values from laboratory data. Sections 4 through 6 present effective stiffness values derived from laboratory test data for C-shaped wall specimens tested as part of this study, for planar wall specimens tested by the authors as part of a previous study, and for non-planar wall specimens tested by others. Section 7 presents the results of a study in which recommended effective stiffness values were used to compute the yield displacements of seven coupled-wall specimens tested in the laboratory by the authors and others. Section 8 summarizes the results of this investigation.

2 Review of Existing Recommendations and Past Research

Design codes, standards of practice and design guidelines typically include reduced, effective stiffness expressions for use in design and evaluation of concrete buildings. These stiffness expressions determine the fundamental period, base-shear demand and lateral drift of the structure under earthquake loading; additionally, the relative stiffness of different building components determines the load distribution within the structure and individual component demands used for design and/or assessment. The effective stiffness expressions included in some design codes, standards of practice and design guidelines are empirically derived expressions. Empirically derived effective stiffnesses are typically defined by the secant stiffness to the measured response envelope at the onset of yielding in the wall.

Table 1 lists the flexural, shear and axial stiffnesses for walls included in nine selected publications. The code-, standard- and guideline-based values are generally limited to a reduction of the flexural stiffness only. One of the recommended flexural stiffnesses included in Table 1 is given as a function of the axial load to account for the increase in stiffness associated with increasing axial load. Most codes of practice acknowledge the presence of shear deformations but do not provide recommendations for reduced shear stiffness; PEER/ATC-72-1 (2010) and Birely (2011) include recommendations for effective shear stiffness. Only CSA A23.3 addresses axial stiffness; a reduction in axial stiffness equal to the reduction in flexural stiffness defined by the upper-bound relationship of Adebar (2007) is recommended.

Recommended stiffnesses in Table 1 are not specific to planar or non-planar walls. For non-planar walls designed per the ACI Code, an effective flange width is prescribed and used to compute the moment of inertia for the section; flexural stiffness is then further reduced per Table 1 to account for concrete

cracking. Similarly the ACI Code prescribes a shear area, and shear stiffness would be reduced per Table 1 to account for concrete cracking.

Table 1: Summary of Various Recommended Effective Stiffness Values for Walls Subjected to Seismic Loading

	ACI 318 (2014)	ASCE 41 (2006)	PEER/ATC-72-1 (2010)	PEER TBI (2010)	NZS: 3101 (2006)	CSA A23.3 (2009)	FIB 27 (2003)	Paulay (2002)	Birely (2011)
Flexure	$\mathbf{0.35E_cI_g - 0.875E_cI_g}$	$\mathbf{0.5E_cI_g}$	$\mathbf{0.4E_cI_g - 0.5E_cI_g}$[1]	$\mathbf{0.75E_cI_g}$[2]	$\mathbf{0.32E_cI_g}$	$\mathbf{(0.6 + P/f_cA_g)E_cI_g}$[3]	$\mathbf{0.3E_cI_g}$	$\mathbf{0.29E_cI_g}$	$\mathbf{0.35E_cI_g}$
Shear			$\mathbf{0.1G_cA_{cv}}$						$\mathbf{0.15G_cA_{cv}}$
Axial						$\mathbf{(0.5 + 0.6P/f_cA_g)E_cA_g}$			

Notes: Values are not provided where gross section stiffness is recommended. 1. Recommendations are for walls with axial loads near 10% of gross-section capacity; for lower axial load levels the lower-bound relationship by Adebar et al. (2007) is recommended. 2. Recommendations for analysis under Service Level Earthquake shaking, for which damage is not expected to limit post-event occupancy of the building. 3. Adebar et al. (2007) upper-bound relationship.

3 Analysis of experimental data

3.1 Calculation of effective stiffness

As part of this study, effective stiffness values for planar and non-planar wall test specimens were determined from experimental data using a Timoshenko beam model. Using this model, a linear vertical strain distribution and constant shear strain distribution are assumed over the wall cross section. Note that this is not recommended for design, but instead used to derive the effective stiffness values from the experimental results. It is presented here for completeness.

Using this model, the effective flexural and shear stiffnesses for a segment of a wall test specimen are defined by the equations below. Birely (2012) derives these equations.

Effective flexural stiffness, EI_{eff}, is defined

$$EI_{eff} = \frac{1}{\theta_{top} - \theta_{bot}} \left[M_{bot} h - \frac{V_{bot} h^2}{2} \right] \tag{1}$$

Effective shear stiffness, GA_{eff}, is defined

$$GA_{eff} = \frac{1}{\kappa} \frac{V_{bot} h}{\Delta_{top} - \Delta_{bot} - \theta_{bot} h - \frac{1}{EI_{eff}} \left[\frac{M_{bot} h^2}{2} - \frac{V_{bot} h^3}{6} \right]} \tag{2}$$

where top and bot refer to the sections at the top and bottom of the wall segment for which effective stiffnesses are being computed, θ_i is the measured rotation at section i of the wall, M_{bot} and V_{bot} are the moment and shear at the bottom section of the wall segment, h is the height of the wall segment, κ is the shear correction factor for the section geometry, and Δ_i is the lateral displacement at section i.

3.2 Calculation of displacement and rotation at the effective height of the wall and calculation of effective wall stiffness.

As part of this study, effective stiffness values were computed using data from multiple test programs. In some tests, the test specimen represented an entire cantilever wall, and shear and axial load only were

applied at the top of the test specimen. In other studies, such as the planar wall tests conducted by Lowes et al. (2012) and the C-shaped wall tests conduct by Behrouzi et al. (2015), the test specimen in the laboratory represented the bottom stories of a cantilever wall, and shear, moment and axial load were applied at the top of the laboratory test specimen.

To enable comparison of stiffness versus drift plots and yield stiffness from different test programs with different loading configurations, average effective stiffnesses were computed assuming a cantilever wall with an effective height. Additionally, plots were constructed of effective stiffness versus drift at the effective height. If only shear and axial loads are applied at the top of the specimen, the height of the applied load is the effective height (this is depicted in Figure 1). If moment, shear and axial load are applied at the top of the specimen, then the effective height of the specimen is defined as

$$h_{eff} = \frac{M_{bot}}{V_{bot}} \tag{3}$$

In the expression, M_{bot} and V_{bot} are the moment and shear at the bottom of the test specimen, as shown in Figure 1. For test specimens for which specimen height does not equal effective height, drift and rotation at the effective height may be computed from i) drift and rotation measured at the top of the laboratory test specimen and ii) assumed flexural and shear stiffness for the portion of the wall not tested in the laboratory. Equations 4 and 5 below define the rotation and displacement at the effective height for a laboratory test specimen of height h_3 that represents the bottom three stories of a taller wall:

$$\theta_{eff} = \theta_3 + \frac{P}{2\alpha_{flex} EI_g}\left(h_{eff} - h_3\right)^2 \tag{4}$$

$$\Delta_{eff} = \Delta_3 + \frac{P}{\kappa\alpha_{shear} GA_g}\left(h_{eff} - h_3\right) + \frac{P}{3\alpha_{flex} EI_g}\left(h_{eff} - h_3\right)^3 + \theta_3\left(h_{eff} - h_3\right) \tag{5}$$

where θ_{eff} and Δ_{eff} are the average rotation and lateral displacement of a wall section at the effective height, θ_3 and Δ_3 are the measured average rotation and lateral displacement at the top of the wall specimen in the laboratory, P is the applied shear load, $\alpha_{flex} EI_g$ is the assumed effective flexural stiffness of the wall above the laboratory test specimen, $\alpha_{hear} GA_g$ is the assumed effective shear stiffness of the wall above the laboratory test specimen, and all other quantities are as previously defined. Figure 1 defines many of these quantities.

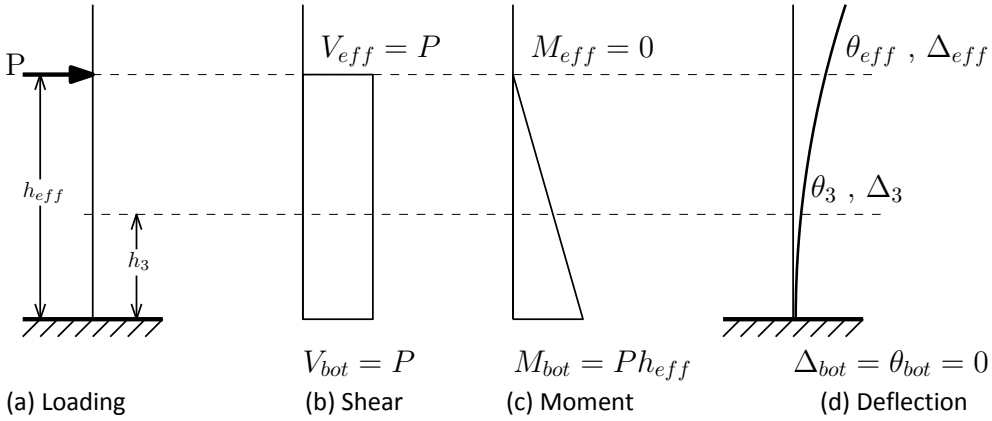

Figure 1: Effective height and rotations and displacements at the top of the specimen and at the effective height

Behrouzi et al. (2015) tested the bottom three stories of a ten-story cantilever wall. Various plausible values for the flexural stiffness modifier, α_{flex}, and shear stiffness modifier, α_{shear}, were used in the above equations to determine the rotation and displacement at the effective height of the ten-story wall.

Figure 2 shows normalized base moment versus computed drift at the tenth story for two sets of effective stiffness; the data show the stiffness modifiers in Equations 4 and 5 have minimal impact on computed displacement. Therefore, subsequent evaluations of the drifts above the third-story were done using 50% of the gross flexural stiffness and 20% of the gross shear stiffness ($\alpha_{flex} = 0.5$, $\alpha_{shear} = 0.2$).

Once rotation and displacement are computed at the effective height of the wall; these data can be used with Equations 1 and 2 to compute effective flexural and shear stiffness for the cantilever wall. These values are appropriate for comparison with similarly computed stiffness values from other test programs.

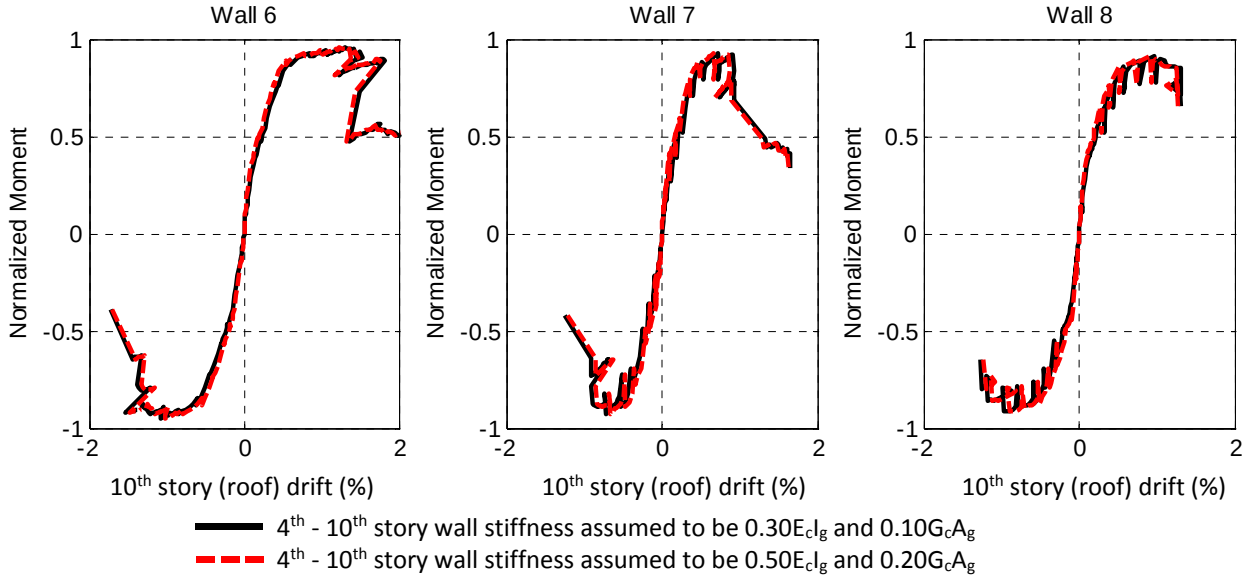

Figure 2: Normalized measured base moment versus computed 10th story (roof) drift for C-shaped walls tested by Behrouzi et al. (2015). The 10th story (roof) drift is computed as the 3rd story drift measured in the laboratory plus the additional drift resulting from flexural and shear deformation of the 4th through 10th stories of the wall, which were not tested in the laboratory. Data show that assumed stiffness for 4th through 10th stories has negligible impact on 10th story (roof) drift.

4 Effective stiffnesses for C-shaped walls tested by Behrouzi et al. (2015)

Effective stiffness values for the C-shaped walls tested by Behrouzi et al. (2015) were determined for both strong and weak-axis loading directions at the maximum and minimum displacement demand levels for each displacement cycle. Stiffnesses were computed for each of the three stories tested in the laboratory and, using the methodology previously described, at the effective height of the walls. Attention is given to the stiffness values for the first story, where most of the damage was observed to occur; attention is also given to the stiffness at the effective height of loading to provide an average stiffness up the height of the cracked wall. Experimental observations and measurements (Behrouzi et al. 2015) indicate significant sliding at the wall-foundation interface under loading activating strong-axis bending as well as significant strain penetration into the foundation for wall vertical reinforcement. The effect of these components of total deformation were determined by calculating the effective stiffness with the base deformations considered as well as the effective stiffness without the base deformations and assuming the base of the wall to be fixed.

The first-story effective stiffness for loading activating strong-axis bending are presented with base deformation excluded (Figure 3) and with base deformation included (Figure 4). As expected, including base deformation results in smaller effective stiffness values. Since base deformations could be expected in all walls and since these deformations would not be included elsewhere within a wall analysis, including base deformation represents a more realistic model for use in elastic analysis. Therefore, the effective stiffness values that are subsequently presented are computed using base deformations. In Figure 3 and Figure 4, effective stiffness flexural and shear stiffness for all three tests are nominally identical for loading in the East and West directions. Therefore, the average of the two stiffnesses for loading in the East and West directions is presented subsequently. Average effective flexural and shear stiffnesses for the first story and the effective height of loading are presented in Figure 5 and Figure 6. Table 2 lists the yield drift and effective flexural and shear stiffnesses (secant stiffnesses to yield) averaged over the effective height of the wall. Note that in Table 2, for the case of strong-axis bending, only the average for the two load directions is provided as loads are applied normal to the axis of symmetry and response in the two directions is approximately the same.

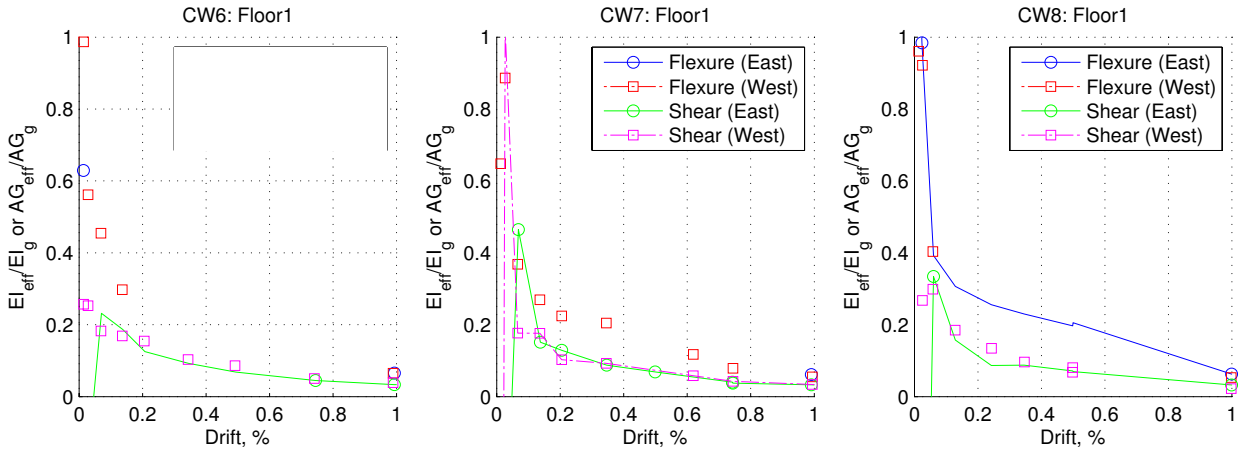

Figure 3: C-shaped wall stiffness at first floor excluding base deformation

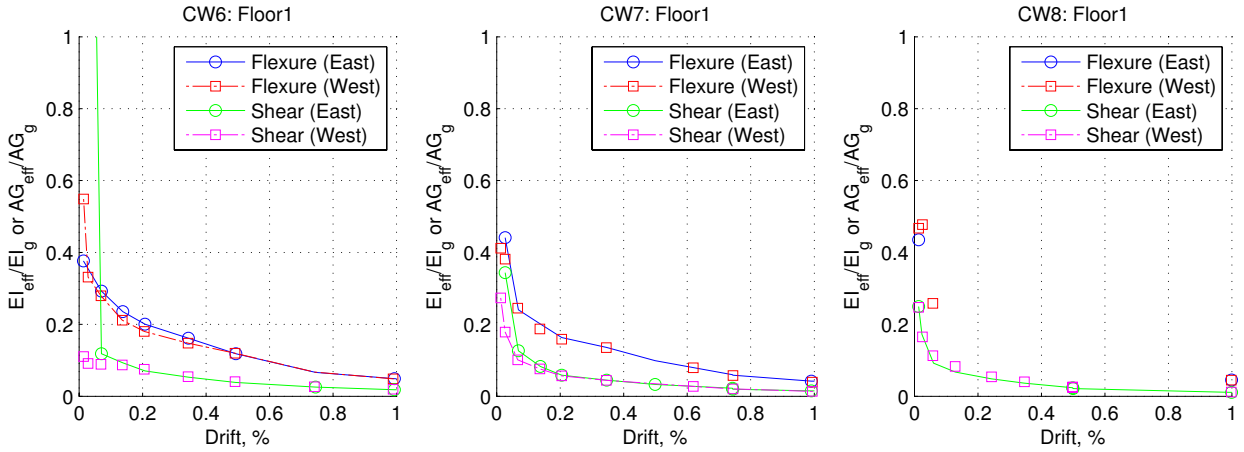

Figure 4: C-shaped wall stiffness at first floor including base deformation and assuming a fixed base

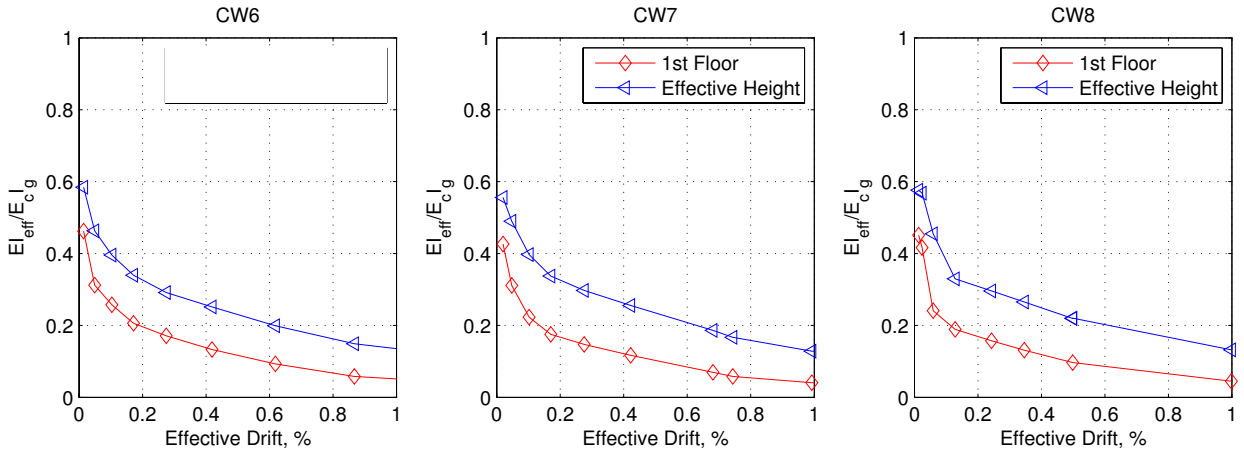

Figure 5: Averaged effective flexural stiffness values for C-shaped walls

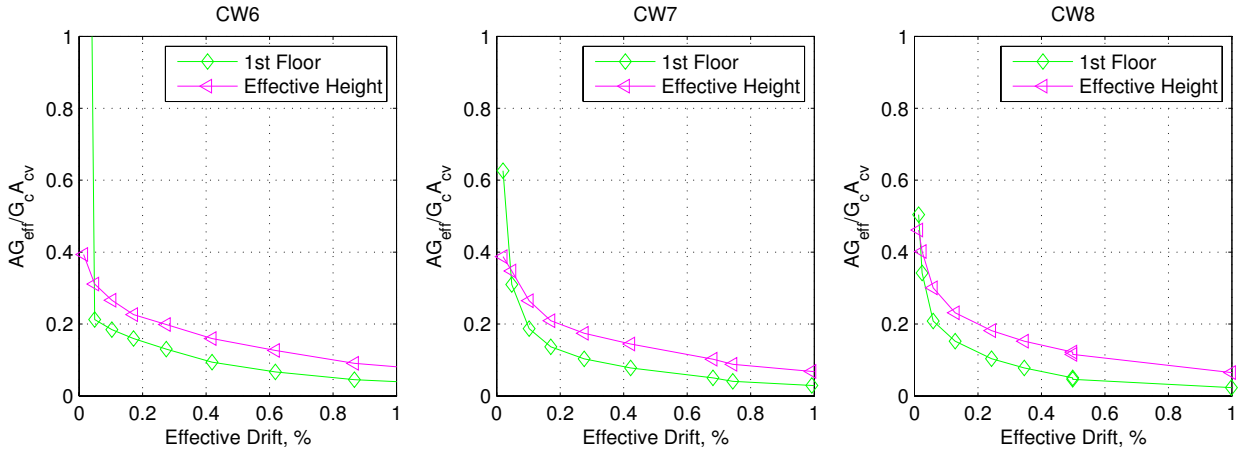

Figure 6: Averaged effective shear stiffness values for C-shaped walls

Table 2: Effective stiffness of C-shaped walls

Wall	Yield Drift	Flexural	Shear
CW6-Strong	0.31%	0.28	0.19
CW7-Strong	0.29%	0.29	0.17
CW8-Strong	0.32%	0.27	0.16
CW7-North	0.96%	0.29	0.07
CW7-South	0.59%	0.26	0.08

Figure 7 presents the average effective stiffness values at the effective height of loading for each C-shaped wall tested by Behrouzi et al. (2015) as well as the effective stiffnesses recommended by PEER/ATC-72-1 and CSA A23.3 Code and the nonlinear effective stiffness models proposed by Brown (2008) and Doepker (2008). With respect to the flexural stiffness, the strong axis response and weak axis response for the web in compression (South) are in close agreement with the nonlinear models. The weak axis response for the toe in compression (North) exhibits a higher effective stiffness with respect to drift. This could be expected given the greater strength in this direction; however, further research is required to determine why toe-

in-tension (South) is consistent with data for strong-axis bending. The flexural stiffness at yield for all directions falls just below the ATC 72 yield definition with an average effective flexural stiffness of $0.28EI_g$.

With respect to the shear stiffness, the strong axis had an average effective shear stiffness at yield of $0.17GA_g$, while the weak axis had an average effective shear stiffness of approximately $0.08GA_g$ at yield. The strong axis response exhibited little deviation between the tests. For the weak axis response prior to yield, loading with the web in compression (South) was less stiff than the strong axis and loading with the toe in compression (North) was stiffer than the strong axis. This is consistent with the flexural stiffness data. Again, further research is required to determine why effective shear stiffness values for weak axis bending are not consistent with those for strong-axis bending.

All three C-shaped walls exhibited little deviation in the effective flexural and shear stiffness for strong-axis bending; thus, bi-directional loading has essentially no impact on the effective stiffness values. Additionally, data are reasonably consistent with the ATC 72 recommendations. Additional tests of bi-directional walls would be needed to evaluate the impact of bi-directional loading on the weak-axis wall response.

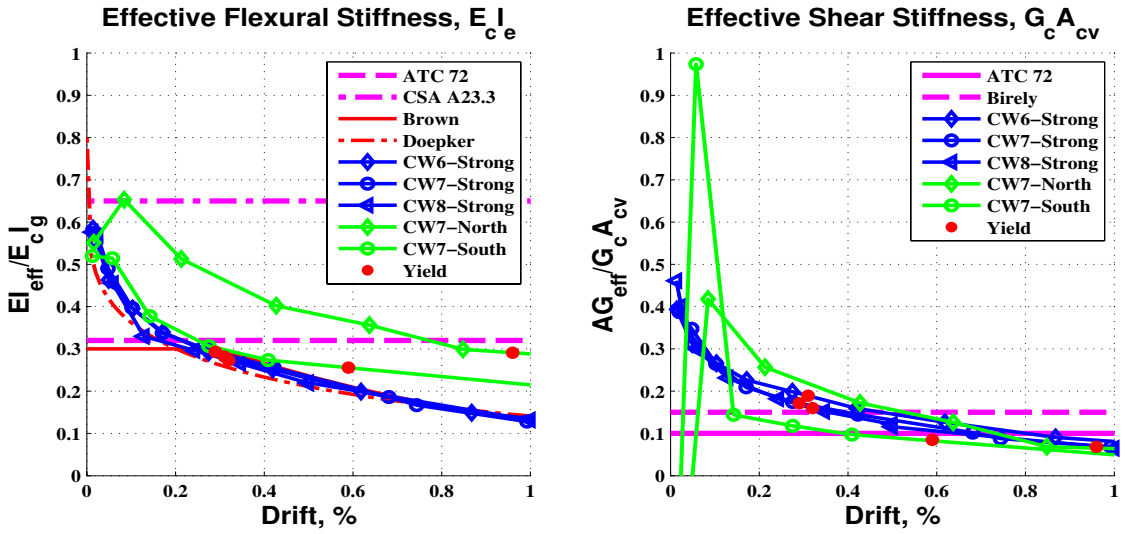

Figure 7: Effective stiffness values of C-shaped walls

5 Effective stiffness of planar walls by Lowes et al. (2012)

Four planar walls with varying reinforcement and loading conditions were tested by Lowes et al. 2012. Effective stiffnesses were computed for these walls using the process and equations presented above. The impact of base deformations on the effective stiffness of planar walls was investigated. In contrast to the C-shaped walls, no significant base sliding was observed for planar wall tests. However, significant rotation at the wall-foundation interface was observed; this was attributed to strain penetration for longitudinal reinforcement anchored into the footing. As with the C-shaped walls, effective stiffness calculations were done with and without base deformation included in calculation. The first-story effective stiffnesses for loading activating strong-axis bending are presented with base deformation ignored in Figure 8 and with base deformation included in Figure 9. As with C-shaped walls, inclusion of base deformation results in lower flexural and shear stiffness values. As with C-shaped walls, inclusion of base deformation was considered to be more appropriate for use in elastic analysis, and effective stiffness values computed including base deformations are reported in Figure 10 and Table 3 below.

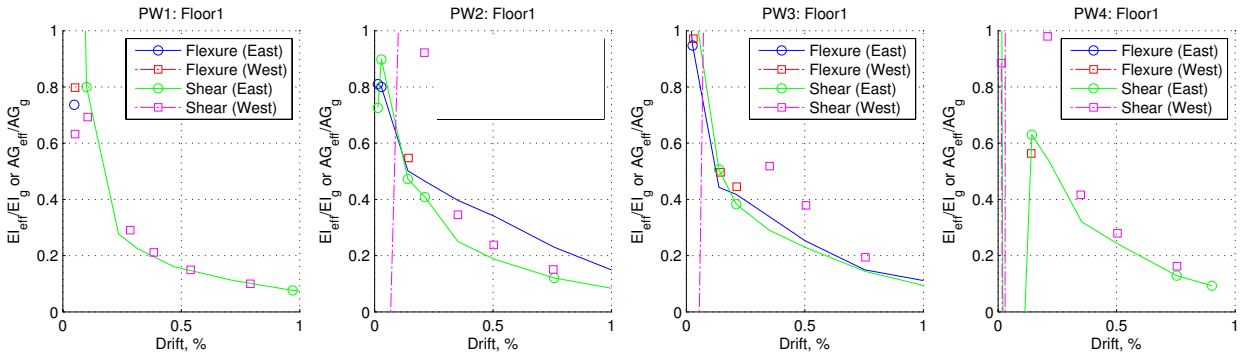

Figure 8: Planar wall first-story effective stiffness with base deformations excluded

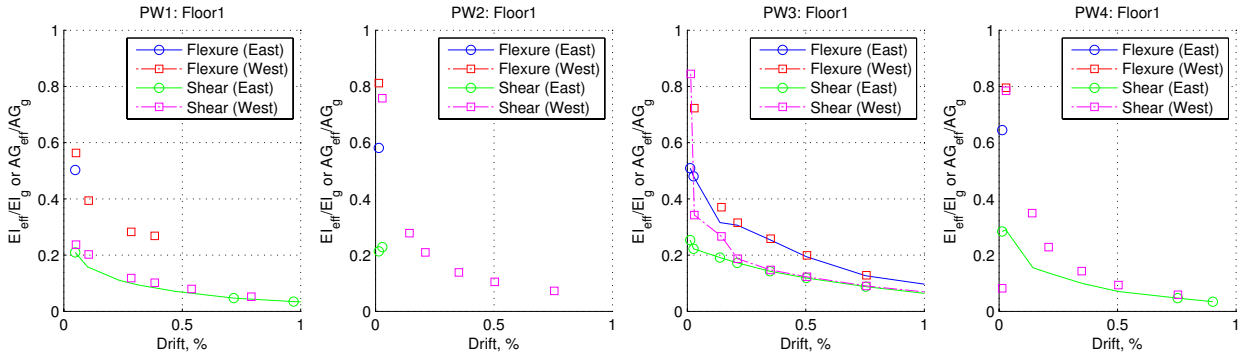

Figure 9 : Planar wall first-story effective stiffness with base deformations included

For all four walls, the effective flexural stiffness is similar for both loading directions. For the first planar wall test (PW1), effective shear stiffness is also approximately the same for both load directions. This was not the case for the remaining tests; for these tests, at low drift levels, shear stiffness was greater for the first half of each load cycle. The first planar wall (PW1) was subjected to a lower shear demand that was used for the subsequent tests. Differences in effective shear stiffness behavior may be due to increased damage due to higher shear demand; damage that accumulates during the first half of the cycle results in increased deformation during the second half of the load cycle and, thus, reduced effective stiffness. However, given limited evidence to support this hypothesis, average effective flexural and shear stiffness values are reported below. Figure 10 presents average effective stiffness versus drift for the planar walls tested by Lowes et al. (2012) as well as values for non-linear models by Brown (2008) and Doepker (2008) and the recommendations provided by ATC 72 and CSA A23.3. The average effective stiffness values at yield are presented in Table 3.

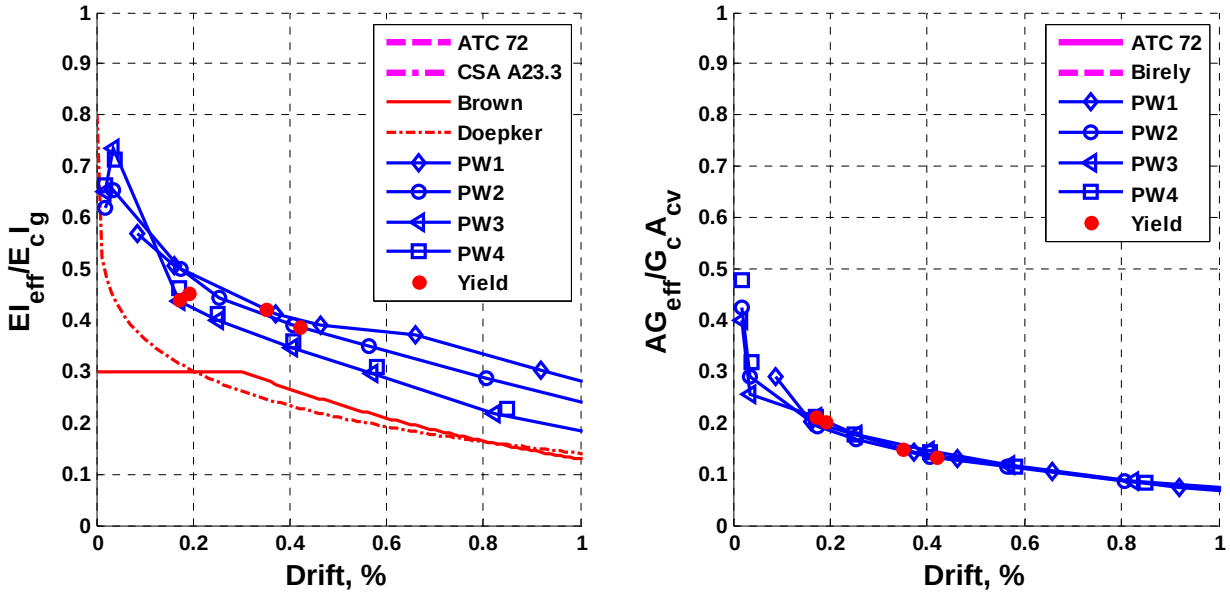

Figure 10: Effective stiffness values of planar walls

Table 3: Effective stiffness of planar walls

Wall	Yield Drift	Flexural	Shear
PW1	0.35%	0.42	0.15
PW2	0.42%	0.39	0.13
PW3	0.17%	0.44	0.21
PW4	0.19%	0.45	0.20

6 Effective stiffness of non-planar walls tested by Beyer et al. (2008) and Oesterle et al. (1976, 1979)

Relatively few researchers measured and reported both displacements and rotations at the top of non-planar wall specimens tested in the laboratory. These data are required to compute effective flexural and shear stiffnesses. These data were provided for U-shaped walls tested by Beyer, Dazio and Priestley (2008) and for the H-shaped walls tested by Oesterle (1976, 1979), and effective stiffness values were computed for these tests using the experimental data provided by the researchers and the methodology described above. Effective stiffness values were calculated at maximum drift demands for each half cycle of loading. For loading perpendicular to axes of symmetry (e.g., bending activating strong-axis loading of C-shaped walls and planar walls), effective stiffness values for the two directions of loading were averaged. Effective stiffness values for walls loaded in directions of asymmetry were reported independently. Effective stiffness versus drift is plotted in Figure 11, and the effective stiffness at first yield is presented in Table 4.

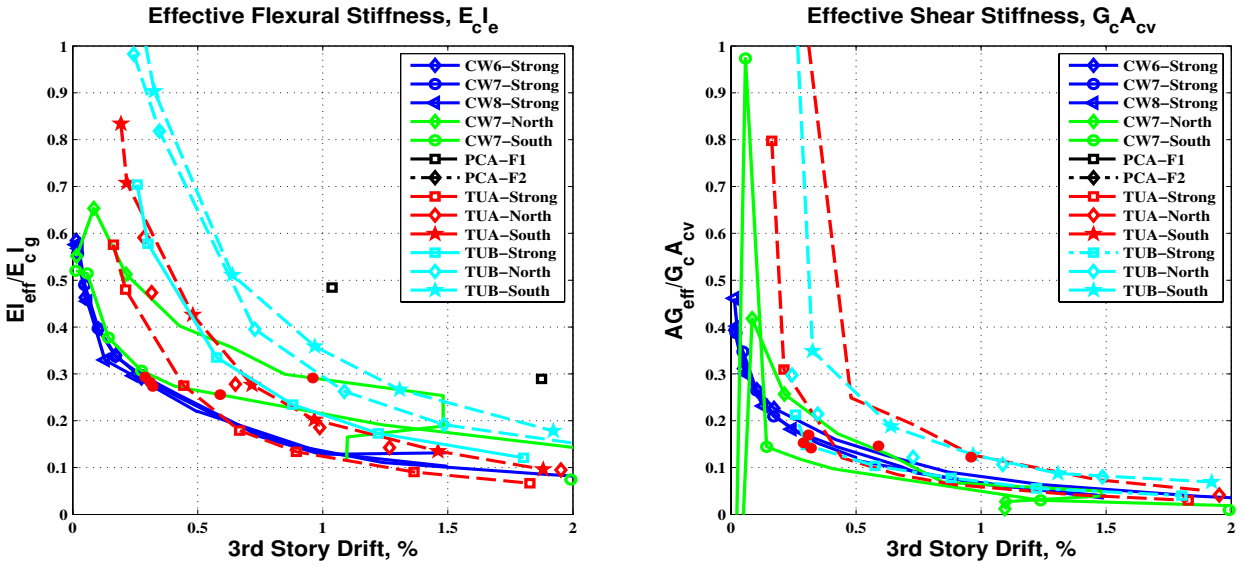

Figure 11: Effective stiffness values for nonplanar walls

Table 4 : Effective stiffness at first yield

Wall	Yield Drift	Flexural	Shear
CW6-Strong	0.31%	0.28	0.19
CW7-Strong	0.29%	0.29	0.17
CW8-Strong	0.32%	0.27	0.16
CW7-North	0.96%	0.29	0.07
CW7-South	0.59%	0.26	0.08
TUA-Strong	0.31%	0.39	0.23
TUA-North	0.33%	0.46	0.18
TUA-South	0.44%	0.47	0.43
TUB-Strong	0.40%	0.49	0.13
TUB-North	0.43%	0.73	0.19
TUB-South	0.51%	0.67	0.25

The data in Figure 11 and Table 4 show variation between the strong and weak directions of the flanged walls. For the data presented in Figure 11, substantially less variability is observed at larger drift demand levels, less variability is observed for shear stiffness than for flexural stiffness, and less variation is observed between specimens in an individual test program. The data in Table 4 support similar observations, with less variability observed for effective shear stiffness than effective flexural stiffness and with less variability observed between specimens in an individual test program, suggesting that variability in the data is not due to entirely to differences in wall configuration but likely results from differences in wall design parameters as well as laboratory test conditions.

7 Effective Stiffnesses Required for Accurate Prediction of the Yield Displacement of Coupled-Wall Test Specimens

To further investigate elastic effective-stiffness modeling of concrete walls, Turgeon applied the effective stiffness recommendations included in ASCE 41 (2007), ACI 318 (2011), CSA A23.3 (2010), NZS 3101

(2006), PEER/ATC 72-1 (2010) as well as the empirically derived effective stiffness values presented by Mohr (2007) for coupling beams and Birely (2012) for planar walls to model the response of seven (7) coupled wall systems tested in the laboratory. All of these specimens were statically indeterminate such that the effective stiffness values used for wall piers and coupling beams determined the load distribution within the specimen. All of the coupled-wall specimens were subjected to unidirectional cyclic lateral loading; a constant axial load was applied to some systems. Five systems included symmetrically reinforced planar (rectangular or barbell) wall piers; one system included asymmetrically reinforced rectangular piers and one system included t-shaped wall piers. Turgeon concluded that the empirically derived effective stiffness recommendations of Birely (2012) and Mohr (2007) and the use of gross-section axial stiffness for wall piers resulted in predictions of loads and deflections at first yield of the system that were significantly better than those predicted using effective stiffness value recommendations included in the design codes, standards of practice and design guidelines listed above. The effective stiffness values found by Turgeon to provide the most accurate prediction of yield displacement for coupled walls tested in the laboratory are listed in Table 5.

Table 5: Recommended Empirically Derived Effective Stiffness Values

Component	Reference Reports	Flexural Rigidity	Shear Rigidity	Axial Rigidity
Coupling Beam	Turgeon (2011), Mohr (2006)	$0.05E_cI_g$	$0.15G_cA_{cv}$	$1.0E_cA_g$
Planar Wall	Turgeon (2011), Birely (2012)	$0.35E_cI_g$	$0.15G_cA_{cv}$	$1.0E_cA_g$
Flanged Wall	Turgeon (2011)	$0.35E_cI_g$	$0.15G_cA_{cv}$	$1.0E_cA_g$

8 Summary

Evaluation of effective flexural and shear stiffness values for the planar and nonplanar walls supports two primary observations:

- Within test programs and for a given wall configuration, effective flexural and shear stiffness are reasonably consistent; however, there is substantial variation in effective stiffness values computed for planar walls tested by Lowes et al. (2012) and C-shaped walls tested by Behrouzi et al. (2015) and for C- and U-shaped walls tested by Behrouzi et al. (2015) and by Beyer et al. (2008). Reduced effective stiffness values for nonplanar walls in comparison with planar walls likely results from more extreme shear distortion of the nonplanar wall cross section. Variability in effective stiffness exhibited by nonplanar wall from different test programs may result from differences in design parameters and/or in test setup. Further research is required to improve understanding of the parameters that determine effective stiffness and to develop methods for more accurate prediction of effective stiffness.

- Bi-directional loading does not impact effective stiffness. Data from test programs in which nominally identical walls were subjected to unidirectional and bidirectional lateral load patterns show that bidirectional loading does not significantly affect response.

- Considering effective stiffness recommendation included in design codes, standards of practice, and design guidelines as well as empirically derived effective stiffness values, the yield displacement of indeterminate coupled-wall specimens tested in the laboratory is most accurately predicted using empirically derived effective stiffness values.

9 Acknowledgements

The research presented herein was funded by the Charles Pankow Foundation and the National Science Foundation through the Network for Earthquake Engineering Simulation Research Program, Grant CMS-042157, Joy Pauschke, program manager. Any opinions, findings, and conclusions or recommendations expressed in this material are those of the authors and do not necessarily reflect the views of the Charles Pankow Foundation or the National Science Foundation.

10 References

ACI Committee 318 (2008). *Building Code Requirements for Structural Concrete (ACI 318-08) and Commentary*. American Concrete Institute, Farmington, IL.

Adebar, P., Ibrahim, A. M. M., and Bryson, M. (2007). "Test of high-rise core wall: Effective stiffness for seismic analysis" *ACI Structural Journal* 104(5): 549-559.

ASCE (2007). *Seismic Rehabilitaion of Existing Buildings. ASCE Standard ASCE/SEI 41-06*, American Society of Civil Engineers, Reston, VA.

Beyer K, Dazio A, Priestley MJN (2008). "Quasi-Static Cyclic Tests of Two U-Shaped Reinforced Concrete Walls," *Journal of Earthquake Engineering* 12:7, 1023-1053.

Birely, Anna C. (2012). "Seismic Performance of Slender Reinforced Concrete Structural Walls". *PhD Dissertation*, University of Washington.

Brown, Peter C. (2008). "Probabilistic Earthquake Damage Prediction for Reinforced Concrete Building Components". *MS Thesis*. University of Washington.

CSA (2004). *Design of Concrete Structures (CSA A23.3-04).* Standards Council of Canada, Toronto, Ontario, Canada (reaffirmed 2010).

Doepker, Blake D. (2008). "Evaluation of Practical Methods for the Evaluation of Concrete Walls". *MS Thesis*. University of Washington.

Federation Internationale du Beton (FIB) (2003). *Seismic design of precast concrete building structures. FIB Bulletin Number 27*. Lausanne, Switzerland

Behrouzi A, Mock A, Lowes LN, Lehman DE, Kuchma DA (2015). "Large-Scale Tests of C-Shaped Reinforced Concrete Walls," Report to Charles Pankow Foundation.

Lowes, L. N., D. E. Lehman, A. C. Birely, D. A. Kuchma, K. P. Marley, and C. R. Hart (2012). "Earthquake Response of Slender Planar Concrete Walls with Modern Detailing." *Engineering Structures* 43: 31–47.

Moehle, J. P., S. Mahin, and Y. Bozorgnia (2010). "Modeling and Acceptance Criteria for Seismic Design and Analysis of Tall Buildings" PEER/ATC-72-1. Applied Technology Council.

NZS (2006). *Concrete Structures Standard, Part 1 - The Design of Concrete Structures, Part 2 - Commentary on the Design of Concrete Structures (3101:2006).* Standards Council, Wellington, New Zealand.

Oesterle RG, Fiorato AE, Johal LS, Carpenter JE, Russell HG, Corely WG (1976). "Earthquake Resistant Structural Walls – Tests of Isolated Walls" *Report to the National Science Foundation for Grant No. GI-43880*. PCI, Skokie, IL.

Oesterle RG, Aristizabal-Ochoa JD, Fiorato AE, Russell HG, Corely WG (1979). "Earthquake Resistant Structural Walls – Tests of Isolated Walls – Phase II" *Report to the National Science Foundation for Grant No. ENV77-15333*. PCI, Skokie, IL.

Paulay, T. (2002). "The displacement capacity of reinforced concrete coupled walls." *Engineering Structures* 24:1165-1175.

Tall Building Guidelines Working Group (2010). "Guidelines for the Performance-Based Seismic Design of Tall Buildings," PEER Report 2010/05.

Thomsen, J., and J. Wallace. 2004. "Displacement-Based Design of Slender Reinforced Concrete Structural Walls—Experimental Verification." *Journal of Structural Engineering* 130 (4): 618–630.